Journal Pre-proof

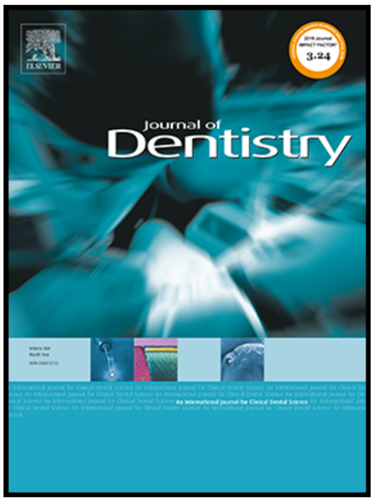

Congruence between the meshes of a combined healing abutment-scan body system acquired with four different intraoral scanners and the corresponding library file: an in vitro analysis

Mustafa Borga Donmez , Vinicius Rizzo Marques , Gülce Çakmak , Hakan Yilmaz , Martin Schimmel , Burak Yilmaz

PII: S0300-5712(21)00360-2
DOI: https://doi.org/10.1016/j.jdent.2021.103938
Reference: JJOD 103938

To appear in: *Journal of Dentistry*

Received date: 29 October 2021
Revised date: 16 December 2021
Accepted date: 19 December 2021

Please cite this article as: Mustafa Borga Donmez , Vinicius Rizzo Marques , Gülce Çakmak , Hakan Yilmaz , Martin Schimmel , Burak Yilmaz , Congruence between the meshes of a combined healing abutment-scan body system acquired with four different intraoral scanners and the corresponding library file: an in vitro analysis, *Journal of Dentistry* (2021), doi: https://doi.org/10.1016/j.jdent.2021.103938

Highlights

1. Intraoral scanners with different scan mechanisms didn't affect the congruence between the library file and the scan mesh of the tested scan body system.

Original article

Full Title: Congruence between the meshes of a combined healing abutment-scan body system acquired with four different intraoral scanners and the corresponding library file: an in vitro analysis

Short title: Congruence of digital implant scans

Authors: Mustafa Borga Donmez, DDS, PhD,[a] Vinicius Rizzo Marques, DDS, MSc, PhD,[b] Gülce Çakmak DDS, PhD,[c] Hakan Yilmaz DDS, MSc,[d] Martin Schimmel DDS, PhD,[e,f] and Burak Yilmaz DDS, PhD[g,h,i]

[a]Assistant Professor, Department of Prosthodontics, Biruni University Faculty of Dentistry, Istanbul, Turkey; bdonmez@biruni.edu.tr

[b]External Researcher, Department of Reconstructive Dentistry and Gerodontology, School of Dental Medicine, University of Bern, Bern, Switzerland; marqvr@gmail.com

[c]Buser Foundation Scholar for Implant Dentistry, Department of Reconstructive Dentistry and Gerodontology, School of Dental Medicine, University of Bern, Bern, Switzerland; guelce.cakmak@zmk.unibe.ch

[d]Orthodontics, Private Practice, Istanbul, Turkey; hakanyilmaz90@gmail.com

[e]Chairman, Department of Reconstructive Dentistry and Gerodontology, School of Dental Medicine, University of Bern, Bern, Switzerland

[f]Privat-Docent extra muros, Division of Gerodontology and Removable Prosthodontics, University Clinics of Dental Medicine, University of Geneva, Geneva, Switzerland; martin.schimmel@zmk.unibe.ch

[g]Associate Professor, Department of Reconstructive Dentistry and Gerodontology, School of Dental Medicine, University of Bern, Bern, Switzerland.

[h]Associate Professor, Department of Restorative, Preventive and Pediatric Dentistry, School of Dental Medicine, University of Bern, Bern, Switzerland; burak.yilmaz@zmk.unibe.ch

[i]Adjunct Professor, Division of Restorative and Prosthetic Dentistry, The Ohio State University College of Dentistry, Ohio, USA.

Corresponding author:

Dr Gülce Çakmak

Department of Reconstructive Dentistry and Gerodontology, University of Bern

Freiburgstrasse 7 3007 Bern, Switzerland

E-Mail: guelce.cakmak@zmk.unibe.ch

ABSTRACT

Objectives: To investigate the congruence between the meshes of a combined healing abutment-scan body (CHA-SB) system acquired with four different intraoral scanners and the corresponding library file.

Material and Methods: A CHA-SB was fixed to an implant at the right first molar position in a dentate mandibular model and digitized by using 4 different intraoral scanners (IOSs) [TRIOS 3 (T3), Omnicam (OC), Primescan (PS), and Virtuo Vivo (VV)] (n=8) and an industrial grade optical scanner (ATOS Core 80) (n=1) to generate standard tessellation language (STL) files of the test scans (CHA-SB-STLs) and the master reference model scan (MRM-STL). A reverse engineering software (Studio Geomagic X) was used to superimpose the proprietary library file of the CHASB over the generated STL files. Root mean square (RMS) values representing the deviations between the library file and the superimposed STL files were statistically analyzed by using 1-way ANOVA (α=.05). Qualitative analysis of the deviations was performed by visual inspection.

Results: Differences between the congruence of the library file and the CHA-SB scans among different IOSs were nonsignificant (F=1.619, df= 3, P = .207). The single best result was 29 ±28.9 µm for OC, 30.8 ±29.6 µm for VV, 35.6 ±35.5 µm for T3, and 39.5 ±39.2

µm for PS, which were all above the deviation value of the scan performed by using the industrial-grade scanner (23.2 ±23.2 µm).

Conclusion: The dimensional congruence between the library file and the standard tessellation language file of the combined healing abutment-scan body system scans was similar when intraoral scanners with different acquisition technologies were used to scan a model with an implant.

Clinical Significance

Scans of the tested intraoral scanners may result in crowns with similar positional accuracy, given the similarities in congruence of their scans with the library file.

Keywords: accuracy, healing abutment-scan body, intraoral scanner, trueness

1. INTRODUCTION

Impression is a critical step in implant-supported prosthetic rehabilitation [1]. Due to the rapid development of computer aided design-computer aided manufacturing (CAD-CAM) and intra oral scanners (IOSs), it is possible to digitize implants in a direct digital workflow [1-3]. This method is performed by scanning intra oral scan bodies (SBs) with an IOS [4] and has improved patient comfort with the elimination of conventional impression materials and trays, eliminates the need for a stone cast, and enables a faster and more efficient communication between the clinician and the laboratory [1, 5-7].

Various types of SBs in different shapes, sizes, surfaces, and connections have been marketed over the years [1, 3]. However, the geometry of a conventional SB or coded healing abutment (HA) generally does not concur with the anatomical shape of a natural tooth [1]. It can also be difficult to accurately position a SB on an apically placed implant with the presence of thick mucosa and repeated removal and placement of an HA in these situations may jeopardize the integrity of the peri-implant soft tissues [1]. Recently introduced combined HA-scan body (CHA-SB) system overcomes these problems as it consists of an HA that contours the peri-implant soft tissue and a SB that is fitted into the screw access hole of the HA. This assembly enables the acquisition of the implant’s position and the soft-tissues simultaneously [3, 10]. Coded (HAs) facilitate digital impressions by reducing the number of appointments to deliver definitive restorations and minimizing the trauma to soft tissues caused by the removal of the HA [8-10]. In addition, potential soft-tissue collapse, which may happen during the removal of a custom HA or interim prosthesis that was used to anatomically shape the peri-implant soft tissues, is eliminated [10].

IOSs depend on different data acquisition mechanisms such as confocal microscopy, optical triangulation, interferometry, active wave front sampling, stereophotogrammetry structured light, laser, and video [2, 4, 11]. Previous studies have shown that a wide range of factors [12, 13], including IOSs, affect the accuracy of a scan [4, 6, 14-21]. However, an accurate scan is only the initial stage of the digital workflow of an implant-supported restoration. After the scan, the SB mesh is replaced with the corresponding CAD file in the library. It is preferable to design the definitive restoration using the CAD library file as it is geometrically optimal, whereas the mesh is an approximation of the scanned data to the actual geometry of the object. A definitive restoration designed by using the library file would lead to improved marginal adaptation [22, 23]. Therefore, dimensional congruence between the library file and the mesh is essential for an optimal restoration [24, 25], and has been investigated only once when different IOSs were used [22]. The SBs evaluated in that study [22] did not include an HA. A previous study has evaluated the accuracy of scans of the new CHA-SB system when 4 different IOSs were used [26], while another study compared the accuracy of CHA-SB scans with a regular scan body [3]. However, those studies [3, 26] did not focus on the dimensional congruence of this system. Considering the limited knowledge on the dimensional congruence of SB meshes with library file and the CHA-SB system in implant dentistry, an investigation combining these two factors could help clinicians to broaden their knowledge on how digital implant scans are processed in the CAD software. Therefore, the purpose of this study was to compare the dimensional congruence between the CHA-SB meshes generated from scans of 4 different IOSs with different data acquisition mechanisms and the CAD library file. The null hypothesis was that the IOS would not affect the dimensional congruence between the CHA-SB meshes generated from 4 different IOS scans and the CAD library file.

2. MATERIALS AND METHODS

2.1. Study Design

Figure 1 summarizes the overall methodology of the present study. A poly(methyl methacrylate) mandibular dentate master model with a single implant (4.0 mm×11 mm, Neoss ProActive Straight; Neoss Implant System, Harrogate, England) at right first molar position was fabricated. The implant was positioned with its inner slot facing buccally for the proper alignment of the HA as per manufacturer's recommendations. The index on the polyetheretherketone (PEEK) HA (Esthetic Healing Abutment, Neoss Implant System, Harrogate, England) was aligned with the buccal groove of the implant and HA was tightened. The SB (ScanPeg, Neoss Implant System, Harrogate, England) was then placed in the screw access hole of the HA [3, 10, 26, 27]. A vertical projection on the SB and a groove present in screw access hole of the HA facilitated this assembly, which was through friction (Figure 2). The components of the CHA-SB system were not disassembled throughout the study.

The master model was digitized by using an industrial optical scanner (ATOS Core 80 5MP; GOM GmbH, Braunschweig, Germany). The industrial scanner depends on the principle of triangulation and has a camera set-up with 6 μm sphere space error, 8 μm size error, 1 μm probing error, 3 μm probing error size, and 7 μm length measurement error [28]. Standard tessellation language (STL) file of the master reference model (MRM-STL) was generated with reverse engineering (Pro 8.1, GOM GmbH, Braunschweig, Germany) [4] and used as the reference.

Four different IOSs were used to scan the CHA-SB system: A confocal microscopy scanning technology IOS: TRIOS 3 (T3) (version 1.4.7.5, 3Shape, Copenhagen, Denmark); an optical triangulation and confocal microscopy technology IOS: Cerec Omnicam (OC) (version 4.6.1, Cerec Dentsply Sirona, Bensheim, Germany); a smart pixel sensor IOS: Cerec Primescan (PS) (version 5.0.0, Cerec-Dentsply Sirona, Bensheim, Germany), and a blue laser IOS with multiscan imaging technology: Virtuo Vivo (VV) (version 3.0, Dentalwings, Montreal, Quebec, Canada). An experienced operator (G. Ç.) with more than 5 years of experience scanned the master model 8 times with each IOS in a humidity and temperature-controlled room under proper ambient light. A priori power analysis (power: 0.80, α: 0.05, and effect size: 0.6) based on the findings in a previous study [4] was performed to determine the number of scans per IOS. The operator rested for 5 minutes in between IOSs to prevent fatigue that may affect the quality of the scans [22]. The IOSs were calibrated before each scan in line with the manufacturers' recommendations. Each scan started from the ipsilateral (the quadrant with the implant) distal molar and the scan strategies were as follows:

T3: The occlusal surface of the entire arch was captured first, followed by the lingual surface scans starting from the contralateral (opposing quadrant to the implant) distal molar. The scan was then completed by scanning the buccal surface starting from the ipsilateral distal molar and terminating at the contralateral distal molar [29].

OC: The scan started with capturing the ipsilateral occlusal surfaces with a 45° tilt of the scanner palatally and terminated at the contralateral lateral incisor. After tilting the scanner by another 45° palatally, the lingual surfaces were scanned. The scanner was then tilted by 90° at the ipsilateral distal molar and occlusal surfaces were scanned moving mesially to the ipsilateral lateral incisor. The buccal surface scans started after a 45° buccal tilt at the contralateral lateral incisor and captured the whole quadrant terminating at the ipsilateral distal molar. Finally, the scanner was tilted by another 45° buccally scanning the buccal surfaces again until the contralateral lateral incisor. The opposite quadrant was also scanned with this sequence [30].

PS: The lingual surfaces of the arch were captured first, followed by the occlusal surface scans starting from the contralateral distal molar. The scan was then completed by buccal surface scans starting from the ipsilateral distal molar and terminating at the contralateral distal molar [31].

VV: Because the manufacturer of this IOS does not recommend a scan path, a scan pattern similar to T3 was used.

Each scan was inspected for imperfections, particularly on SB surfaces. A scan was considered complete when no major imperfections were detected [7]. IOS scans (test scans) were converted to STL files to generate CHA-SB meshes (CHA-SB-STL). In total, 33 STL files (32 CHA-SB-STLs and 1 MRM-STL) were collected. CHA-SB system's proprietary library CAD file, provided by the manufacturer, was used as the reference STL (nominal, CAD-LIB-STL) to simulate the generation of an implant CAD model.

2.2. Deviation Analysis

A reverse engineering software (Studio Geomagics v.2018.1.1, Morrisville, NC, USA) was used to measure the dimensional congruence between the CHA-SB-STLs and the CAD-LIB-STL by using the best-fit algorithm. Root mean square (RMS) was utilized to indicate the magnitude of deviations from zero between the 2 datasets (CHA-SB-STLs and the CAD-LIB-STL) [32]. A high RMS value indicated a low-degree of 3D matching in superimposed files of the CHA-SB system, which translated to low trueness [33].

All CHA-SB-STLs and the CAD-LIB-STLs were imported into the software. CAD-LIB-STL was used as the reference data. For the initial alignment, "Transform Alignment Function" of the software with N points method was used. Three different points (one point on the buccal vertical outdent on the SB and HA connection area, one point on the buccal of the triangle located on top of the SB, and one point on the distal of the triangle located on top of the SB) were identified on both the CHA-SB-STLs and the CAD-LIB-STL for the superimposition (Figure 3). Then the "Best-Fit Alignment" function of the software was used for further alignment and to minimize errors.

For the quantitative (mean ± standard deviation (SD)) and qualitative (inward and outward, and minimal deviations) evaluation of the deviations between the CHA-SB-STLs and the CAD-LIB-STLs, color-difference maps were created by using "3D Comparison Function" of the software. The color-difference maps allowed the evaluation of the distances between specific points, globally and in x, y, and z planes. The maximum/minimum deviation values were arranged to be +50/-50 µm, the tolerance range being +10/-10 µm (green) [34]. One experienced operator (V.R.) with 5 years of experience on digital dental technologies and 3D analysis software performed the evaluations.

2.3. Statistical Analysis

For the quantitative evaluation, the software automatically calculated the RMS in color difference maps, without the need for an additional formula. Minimum, maximum, average deviations, RMS, standard deviation (µm), and total deviation percentage (%) values were recorded for each test scan. The same procedure was done for the MRM-STL. The data were analyzed by using 1-way analysis of variance (ANOVA) ($\alpha = 0.05$).

Qualitative evaluation was performed to understand the direction of the deviation (inward or outward) and to determine if there was minimal deviation. Screenshots were made from different angles after the best-fit alignment and color-difference map generation to visually evaluate the parts of the CHA-SB system individually and as a whole. Similar to the quantitative evaluation, CAD-LIB-STL was accepted as the reference and the same experienced operator (V.R.) executed the qualitative evaluation. The deviations were recorded for buccal, lingual, and occlusal surfaces according to the chromatic existence of red/yellow, green, or light/dark blue in color difference maps. The data of the occlusal surface were included in the analysis of the SB. Different shades of blue indicated Inward deviations (defects) and yellow, orange, and red indicated the outward deviations (excesses) [22]. Green indicated no deviation. The results were expressed as a qualitative variable.

3. RESULTS

One-way ANOVA revealed that there were no significant differences among the dimensional congruence of the CHA-SB system scans performed with different IOSs ($F=1.619$, $df= 3$, $P= .207$). Table 1 summarizes the descriptive statistics of the scans performed by using the tested IOSs, while the results of the pairwise comparisons are shown in Table 2.

Figure 4 illustrates the color maps generated to analyze the congruence between the CHA-SB mesh and the library CAD file for each IOS. The best single result (lowest deviation value among the scans performed) was 35.6 ±35.5 μm for T3, 29 ±28.9 μm for OC, 39.5 ±39.2 μm for PS, and 30.8 ±29.6 μm for VV. The reference scan superimposition over the library CAD file resulted in 23.2 ±23.2 μm of deviation, which was below the best single results from all IOSs tested.

Table 3 summarizes the qualitative evaluation of the deviations of the CHA-SB system scans made by visual inspection. The scans performed by using T3 mainly resulted in deviations that were within the tolerance range. However, inward deviations were observed on the lingual surfaces of the complete CHA-SB system and the SB. When scanned with OC, CHA-SB system showed both inward deviations or deviations within the tolerance range. For the HA, deviations were within the tolerance for both lingual and buccal surfaces, and inward deviations were observed on the buccal surface. For the SB, an inward deviation was predominant for each surface (buccal, lingual, and occlusal), and deviations within the tolerance range were also observed on the occlusal surface. When PS was used, the deviations observed on the buccal and lingual surfaces of the complete CHA-SB system, the HA, and the SB were mainly inward or deviations within the tolerance range. For the occlusal surface of the SB, deviations were predominantly within the tolerance range. When VV was utilized, scans of the complete CHA-SB system, HA, and SB mostly showed outward deviations or deviations within the tolerance range for buccal and lingual surfaces. For the occlusal surface of the SB, deviations were mainly within the tolerance range.

4. DISCUSSION

The scans of the CHA-SB system performed by using different IOSs resulted in similar deviations when superimposed over the library CAD file. Therefore, the null hypothesis was accepted.

A recent study investigated the dimensional congruence between the scans of an edentulous maxilla rehabilitated with 6 implants (#16, #14, #11, #21, #24, and #26) and library file [22]. The authors [22] reported significant differences among 5 IOSs (Primescan, CS3700, MEDIT i-500, ITERO ELEMENTS 5D, and Emerald S) and 1 desktop scanner (Freedom UHD) as well as different implant positions. Among the IOSs tested, PS resulted in the highest congruence (25.5 ±5 µm) with the library CAD file, which was similar to the deviation value of the desktop scanner (25.5 ±2.9 µm) and CS3700 (27 ±4.3 µm). Moreover, PS showed the single best result (lowest) (17 ±19 µm) when compared with the other scanners quantitatively. The implant positions were also found to be effective on the dimensional congruence of the scans. The mean deviation values in scans performed by using PS ranged from 22.2 to 31 µm, SBs located at the right first premolar, left first premolar, and left first molar showing significantly higher trueness than the other SBs. The contrasting results between the present study and Mangano et al's [22] study might be related to several factors, one of which is the anatomy of the SB [1]. The CHA-SB system is more complex than a conventional SB as it consists of 2 individual parts that are assembled through friction fit and these 2 pieces are geometrically different [3, 10, 26]. The SBs used in Mangano et al's [22] study were 1-piece, which had a more uniform geometry than that of the CHA-SB system. In addition, the authors [22] stated that the flat surfaces of nearly all SBs showed the lowest deviation results. The absence of a flat surface on the CHA-SB system might have led to the higher deviation values observed in the present study. Other factors, which may have contributed to the higher deviation values in the present study are operator difference [21], scan pattern [24, 35-38], ambient light [39], and the differences in IOSs tested [4, 6, 15-19] other than PS. Nonetheless, considering that different IOSs resulted in similar deviations, it can be speculated that definitive restorations manufactured by using these scans would also have similar positional trueness. However, this hypothesis needs further support with studies evaluating the fit and the contours (interproximal and occlusal contacts) of definitive crowns fabricated when the CHA-SB system scans are used.

Effect of IOSs on the scan accuracy of CHA-SB system was investigated in a previous study, in which IOSs tested in the present study were evaluated [26]. It was concluded that the IOSs did not affect the distance deviations of the scans, which is in line with the present study. These results might be attributed to the anatomy of the master model as it contained only one implant and no edentulous spaces. Previous studies have shown that increasing the number of implants and edentulous spaces [18, 40] led to higher deviations. Thus, different clinical situations might result in differences among different IOSs. Furthermore, the mean distance deviations reported (127 μm for T3, 124.6 μm for OC, 126.6 μm for PS, and 105.3 for VV) [26] were above the findings of the present study. However, careful interpretation of these results is necessary, since the deviation data in Çakmak et al's [26] study was based on a comparison between the scans of an industrial-grade scanner and the IOSs. The congruence between the master model mesh generated from the scan of an industrial-grade scanner and library CAD file was also evaluated in the aforementioned study to verify the fit between the HA and the SB [26]. Even though the deviation values in the present study are higher than the reported master model distance deviation (4.4 μm), a direct comparison would be misleading due to the differences in analysis and software used [41-43]. Çakmak et al [26] generated two circular planes (one at the top of the SB and one 3 mm below) that are parallel to each other in both master CHA-SB mesh and library file and calculated the linear deviations of the center points of the circles below in x, y, and z axes. Additionally, the 3D analysis software used in Çakmak et al's [26] study (GOM Inspect) had prealignment feature for the initial alignment of the data, which was then followed by the best-fit alignment.

In another study, which compared the accuracy of scans of an anterior implant digitized either by the CHA-SB system or a conventional SB (direct and indirect workflow), similar deviation results were reported [3]. However, taking into account that CHA-SB system is a new approach in digital implant dentistry, future studies investigating different factors that might affect the scan accuracy are needed to broaden the knowledge on this system. Moreover, previous studies have shown that the accuracy of an implant scan might be affected by the manufacturing tolerances of the SBs [25, 44] as various materials are used for the fabrication of SBs [1]. Schmidt et al [25] compared the manufacturing tolerances of 3 SBs by using x-ray computed tomography and concluded that the scan accuracy might be affected by manufacturing tolerances. These findings were corroborated in a previous study [44], where different 1-piece SBs were investigated. The highest tolerances and deviations were found in vertical direction with implants that had conical connections. Unlike conventional SBs, CHA-SB has 2 pieces, which are composed of different materials. Therefore, the manufacturing tolerances of the CHA-SB system may affect the scan accuracy more significantly, which should be investigated in future studies.

This in vitro study was performed under standardized conditions. Therefore, factors like gag reflex, presence of blood or saliva, space limitation, and patient movement, which may affect the scan accuracy in clinical practice were excluded [2, 6, 7, 18]. The present study focused on the influence of IOSs on the scan accuracy of the CHA-SB system. Given the fact that the scan accuracy is affected by various factors such as the type of the IOS, the experience of the operator, the scan strategy, and the ambient light [13, 18, 21, 24, 35-39] and the present study being the first on the dimensional congruence of the CHA-SB system scans, future studies should elaborate the findings of the present study by investigating the angular deviations of the CHA-SB system scans as well as the precision of these scans when performed by different operators.

5. CONCLUSIONS

Considering the limitations of the present study, the results suggest that the congruence between the CHA-SB scans and CAD library file was similar when tested IOSs were used. However, future studies are necessary to corroborate and to elaborate these preliminary findings, as the effect of the level of congruence between the CHA-SB scans and CAD library file on the fabricated restorations are unknown.

Author Statement

The authors of the manuscript contributed in the following ways to the submitted manuscript:

Mustafa Borga Donmez: Design, Data collection, Drafting article

Vinicius Rizzo Marques: Data collection, Data interpretation

Gülce Çakmak: Design, Data collection, Drafting article, Critical revision of article

Hakan Yilmaz: Data analysis, Data interpretation, Statistical analysis.

Martin Schimmel: Design, Critical revision of article

Burak Yilmaz: Data interpretation, Critical revision of the article, Approval of the submitted and final versions

Declaration of interests

☒ The authors declare that they have no known competing financial interests or personal relationships that could have appeared to influence the work reported in this paper.

Acknowledgement

All other authors have no conflicts of interest to declare. The authors do not have any financial interest in the companies whose materials are included in this article.

Neoss Implant System is gratefully acknowledged for supplying the materials used in this study. The authors also thank Gökhan Akcagöz for supplying the materials.

REFERENCES

[1] R.M. Mizumoto, B. Yilmaz, Intraoral scan bodies in implant dentistry: A systematic review, J Prosthet Dent 120(3) (2018) 343-352. https://doi.org/10.1016/j.prosdent.2017.10.029

[2] R.M. Mizumoto, B. Yilmaz, E.A. McGlumphy, Jr., J. Seidt, W.M. Johnston, Accuracy of different digital scanning techniques and scan bodies for complete-arch implant-supported prostheses, J Prosthet Dent 123(1) (2020) 96-104. https://doi.org/10.1016/j.prosdent.(2019).01.003

[3] B. Yilmaz, D. Gouveia, V.R. Marques, E. Diker, M. Schimmel, S. Abou-Ayash, The accuracy of single implant scans with a healing abutment-scanpeg system compared with the scans of a scanbody and conventional impressions: an in vitro study, Journal of Dentistry (2021) 103684. https://doi.org/10.1016/j.jdent.2021.103684.

[4] G. Çakmak, H. Yilmaz, A. Treviño, A.M. Kökat, B. Yilmaz, The effect of scanner type and scan body position on the accuracy of complete-arch digital implant scans, Clin Implant Dent Relat Res 22(4) (2020) 533-541. https://doi.org/10.1111/cid.12919

[5] F. Mangano, A. Gandolfi, G. Luongo, S. Logozzo, Intraoral scanners in dentistry: a review of the current literature, BMC Oral Health 17(1) (2017) 149. https://doi.org/10.1186/s12903-017-0442-x.

[6] F.G. Mangano, O. Admakin, M. Bonacina, H. Lerner, V. Rutkunas, C. Mangano, Trueness of 12 intraoral scanners in the full-arch implant impression: a comparative in vitro study, BMC Oral Health 20(1) (2020) 263. https://doi.org/10.1186/s12903-020-01254-9.

[7] R.M. Mizumoto, G. Alp, M. Özcan, B. Yilmaz, The effect of scanning the palate and scan body position on the accuracy of complete-arch implant scans, Clin Implant Dent Relat Res 21(5) (2019) 987-994. https://doi.org/10.1111/cid.12821.

[8] J. Abduo, C. Chen, E. Le Breton, A. Radu, J. Szeto, R. Judge, I. Darby, The effect of coded healing abutments on treatment duration and clinical outcome: a randomized controlled clinical trial comparing encode and conventional impression protocols, Int J Oral Maxillofac Implants 32(5) (2017) 1172–1179. https://doi.org/10.11607/jomi.5386.

[9] D.H. Mahn, T. Prestipino, CAD/CAM implant abutments using coded healing abutments: a detailed description of the restorative process, Compend Contin Educ Dent 34(8) (2013) 612-615.

[10] B. Yilmaz, S. Abou-Ayash, A digital intraoral implant scan technique using a combined healing abutment and scan body system, J Prosthet Dent 123(2) (2020) 206-209. https://doi.org/10.1016/j.prosdent.2019.01.016.

[11] S. Logozzo, E.M. Zanetti, G. Franceschini, A. Kilpelä, A. Mäkynen, Recent advances in dental optics – Part I: 3D intraoral scanners for restorative dentistry, Opt Lasers Eng 54 (2014) 203-221. https://doi.org/10.1016/j.optlaseng.2013.07.017.

[12] B. Yilmaz, V. Rizzo Marques, X. Guo, D. Gouveia, S. Abou-Ayash, The effect of scanned area on the accuracy and time of anterior single implant scans: An in vitro study, J Dent (2021) 103620. https://doi.org/10.1016/j.jdent.2021.103620.

[13] M. Revilla-León, Z. Smith, M.M. Methani, A. Zandinejad, M. Özcan, Influence of scan body design on accuracy of the implant position as transferred to a virtual definitive implant cast, J Prosthet Dent (2020). https://doi.org/10.1016/j.prosdent.2020.03.019.

[14] M. Braian, A. Wennerberg, Trueness and precision of 5 intraoral scanners for scanning edentulous and dentate complete-arch mandibular casts: A comparative in vitro study, J Prosthet Dent 122(2) (2019) 129-136.e2. https://doi.org/10.1016/j.prosdent.2018.10.007.

[15] M. Imburgia, S. Logozzo, U. Hauschild, G. Veronesi, C. Mangano, F.G. Mangano, Accuracy of four intraoral scanners in oral implantology: a comparative in vitro study, BMC Oral Health 17(1) (2017) 92. https://doi.org/10.1186/s12903-017-0383-4.

[16] R.J. Kim, G.I. Benic, J.M. Park, Trueness of digital intraoral impression in reproducing multiple implant position, PLoS One 14(11) (2019) e0222070. https://doi.org/10.1371/journal.pone.0222070.

[17] R.J.Y. Kim, G.I. Benic, J.M. Park, Trueness of ten intraoral scanners in determining the positions of simulated implant scan bodies, Sci Rep 11(1) (2021) 2606. https://doi.org/10.1038/s41598-021-82218-z.

[18] F.G. Mangano, U. Hauschild, G. Veronesi, M. Imburgia, C. Mangano, O. Admakin, Trueness and precision of 5 intraoral scanners in the impressions of single and multiple implants: a comparative in vitro study, BMC Oral Health 19(1) (2019) 101. https://doi.org/

[19] F.G. Mangano, G. Veronesi, U. Hauschild, E. Mijiritsky, C. Mangano, Trueness and Precision of Four Intraoral Scanners in Oral Implantology: A Comparative in Vitro Study, PLoS One 11(9) (2016) e0163107. https://doi.org/10.1186/s12903-019-0792-7.

[20] C.C.D. Resende, T.A.Q. Barbosa, G.F. Moura, L.D.N. Tavares, F.A.P. Rizzante, F.M. George, F.D.D. Neves, G. Mendonça, Influence of operator experience, scanner type, and scan size on 3D scans, J Prosthet Dent 125(2) (2021) 294-299. https://doi.org/10.1016/j.prosdent.2019.12.011.

[21] G. Revell, B. Simon, A. Mennito, Z.P. Evans, W. Renne, M. Ludlow, J. Vág, Evaluation of complete-arch implant scanning with 5 different intraoral scanners in terms of trueness and operator experience, J Prosthet Dent (2021). https://doi.org/10.1016/j.prosdent.2021.01.013.
[22] F. Mangano, H. Lerner, B. Margiani, I. Solop, N. Latuta, O. Admakin, Congruence between meshes and library files of implant scanbodies: an in vitro study comparing five intraoral scanners, J Clin Med 9(7) (2020) 2174. https://doi.org/10.3390/jcm9072174.
[23] H. Lerner, J. Mouhyi, O. Admakin, F. Mangano, Artificial intelligence in fixed implant prosthodontics: a retrospective study of 106 implant-supported monolithic zirconia crowns inserted in the posterior jaws of 90 patients, BMC Oral Health 20(1) (2020) 80. https://doi.org/10.1186/s12903-020-1062-4.
[24] C. Motel, E. Kirchner, W. Adler, M. Wichmann, R.E. Matta, Impact of different scan bodies and scan strategies on the accuracy of digital implant impressions assessed with an intraoral scanner: an in vitro study, J Prosthodont 29(4) (2020) 309-314. https://doi.org/10.1111/jopr.13131.
[25] A. Schmidt, J.W. Billig, M.A. Schlenz, P. Rehmann, B. Wöstmann, Influence of the accuracy of intraoral scanbodies on implant position: differences in manufacturing tolerances, Int J Prosthodont 32(5) (2019) 430-432. https://doi.org/10.11607/ijp.6371.
[26] G. Çakmak, M.B. Donmez, S. Atalay, H. Yilmaz, A.M. Kökat, B. Yilmaz, Accuracy of single implant scans with a combined healing abutment-scan body system and different intraoral scanners: An in vitro study, J Dent 113 (2021) 103773. https://doi.org/10.1016/j.jdent.2021.103773.
[27] Neoss Implant System Website. https://resources.neoss.com/uploads/11926_3-IFUEsthetic- Healing-Abutments-with-ScanPeg-EN-spread-PRINTINT. pdf?mtime=20210330102135. Accessed April 14, 2021.
[28] GOM: ATOS Core - Features. https://www.atos-core.com/en/features.php#3dScanning. Accessed July 24, 2021.
[29] The 3Shape Web Site https://3shape.widen.net/view/pdf/xt7bnel76t/TRIOS-UserManual-2015-1-1.4.7.0-A-EN.pdf?t.download=true&u=6xmdhr accessed on 21.04.2021
[30] The Sirona web site, https://manuals.sirona.com/en/digital-dentistry/cerec-chairsidesolutions/ cerec-omnicam-ac accessed on 21.04.2021
[31] The Sirona web site, https://manuals.sirona.com/en/digital-dentistry/cerec-chairsidesolutions/ cerec-primescan-ac accessed on 21.04.2021
[32] O. Schaefer, D.C. Watts, B.W. Sigusch, H. Kuepper, A. Guentsch, Marginal and internal fit of pressed lithium disilicate partial crowns in vitro: a three-dimensional analysis of

accuracy and reproducibility, Dent Mater 28(3) (2012) 320-6. https://doi.org/10.1016/j.dental.2011.12.008.

[33] International Organization for Standardization. ISO-5725-2. Accuracy (trueness and precision) of measurement methods and results-part 2: basic method for the determination of repeatability and reproducibility of a standard measurement method. Geneva: ISO; 1994. Available at: http://www.iso. org/iso/store.htm. Last accessed December 22, 1994

[34] W. Wang, H. Yu, Y. Liu, X. Jiang, B. Gao, Trueness analysis of zirconia crowns fabricated with 3-dimensional printing, J Prosthet Dent 121(2) (2019) 285-291. https://doi.org/10.1016/j.prosdent.2018.04.012.

[35] J. Latham, M. Ludlow, A. Mennito, A. Kelly, Z. Evans, W. Renne, Effect of scan pattern on complete-arch scans with 4 digital scanners, J Prosthet Dent 123(1) (2020) 85-95. https://doi.org/10.1016/j.prosdent.2019.02.008.

[36] A.S. Mennito, Z.P. Evans, A.W. Lauer, R.B. Patel, M.E. Ludlow, W.G. Renne, Evaluation of the effect scan pattern has on the trueness and precision of six intraoral digital impression systems, J Esthet Restor Dent 30(2) (2018) 113-118. https://doi.org/10.1111/jerd.12371.

[37] K.C. Oh, J.M. Park, H.S. Moon, Effects of scanning strategy and scanner type on the accuracy of intraoral scans: a new approach for assessing the accuracy of scanned data, J Prosthodont 29(6) (2020) 518-523. https://doi.org/10.1111/jopr.13158.

[38] L. Passos, S. Meiga, V. Brigagão, A. Street, Impact of different scanning strategies on the accuracy of two current intraoral scanning systems in complete-arch impressions: an in vitro study, Int J Comput Dent 22(4) (2019) 307-319.

[39] M. Revilla-León, P. Jiang, M. Sadeghpour, W. Piedra-Cascón, A. Zandinejad, M. Özcan, V.R. Krishnamurthy, Intraoral digital scans-Part 1: Influence of ambient scanning light conditions on the accuracy (trueness and precision) of different intraoral scanners, J Prosthet Dent 124(3) (2020) 372-378. https://doi.org/10.1016/j.prosdent.2019.06.003.

[40] L. Canullo, M. Colombo, M. Menini, P. Sorge, P. Pesce, Trueness of intraoral scanners considering operator experience and three different implant scenarios: a preliminary report, Int J Prosthodont 34(2) (2021) 250–253. https://doi.org/10.11607/ijp.6224.

[41] G.H. Park, K. Son, K.B. Lee, Feasibility of using an intraoral scanner for a complete-arch digital scan, J Prosthet Dent 121(5) (2019) 803-810. https://doi.org/10.1016/j.prosdent.2018.07.014.

[42] B. Batak, B. Yilmaz, K. Shah, R. Rathi, M. Schimmel, L. Lang, Effect of coded healing abutment height and position on the trueness of digital intraoral implant scans, J Prosthet Dent 123(3) (2020) 466-472. https://doi.org/10.1016/j.prosdent.2019.06.012.
[43] K. Son, W.S. Lee, K.B. Lee, Effect of different software programs on the accuracy of dental scanner using three-dimensional analysis, Int J Environ Res Public Health 18(16) (2021) 8449. https://doi.org/10.3390/ijerph18168449.
[44] H. Lerner, K. Nagy, F. Luongo, G. Luongo, O. Admakin, F.G. Mangano, Tolerances in the production of six different implant scanbodies: a comparative study, Int J Prosthodont 34(5) (2021) 591-599. https://doi.org/10.11607/ijp.7379.

TABLES

Table 1. Descriptive statistics of the CHA-SB scans performed with each IOS

IOS	Mean ±standard deviation (µm)	Min-Max deviation (µm)	95 % CI (µm)
T3	37.8 ±2.4	35.6-41.6	35.8-39.8
OC	42.1 ±13.8	29-68.7	30.6-53.7
PS	40.4 ±0.6	39.5-42.9	39.9-40.9
VV	34.7 ±3.2	30.8-55.5	32-41.4

Table 2. *P* values of the pairwise comparisons

IOS	T3	OC	PS	VV
T3	-	.627	.885	.827
OC	.627	-	.963	.19
PS	.885	.963	-	.404
VV	.827	.19	.404	-

$P<.05$ indicate significant differences among groups

Table 3. Distribution of the deviations on each surface of the combined healing abutment-scan body system

		Deviation	Lingual	Buccal	Occlusal
T3	CHA-SB	Inward	++	+	
		Outward	+	+	
		No	+	++	
	HA	Inward	+	+	
		Outward	+	+	
		No	++	++	
	SB	Inward	++	+	+
		Outward	+	+	+
		No	++	++	++
			Lingual	Buccal	Occlusal
OC	CHA-SB	Inward	++	++	
		Outward	+	+	
		No	++	++	
	HA	Inward	+	++	
		Outward	+	+	
		No	++	++	
	SB	Inward	++	++	++
		Outward	+	+	+
		No	+	+	++
			Lingual	Buccal	Occlusal
PS	CHA-SB	Inward	++	++	
		Outward	+	+	
		No	+++	++	
	HA	Inward	++	++	
		Outward	+	+	
		No	++	++	
	SB	Inward	++	++	+
		Outward	++	+	++
		No	++	++	+++
			Lingual	Buccal	Occlusal
VV	CHA-SB	Inward	+	+	
		Outward	++	+	
		No	+++	+++	
	HA	Inward	+	+	
		Outward	++	++	
		No	+++	+++	
	SB	Inward	+	+	+
		Outward	++	++	+
		No	+++	+++	+++

* +: Less; ++: Normal; +++: More

FIGURES

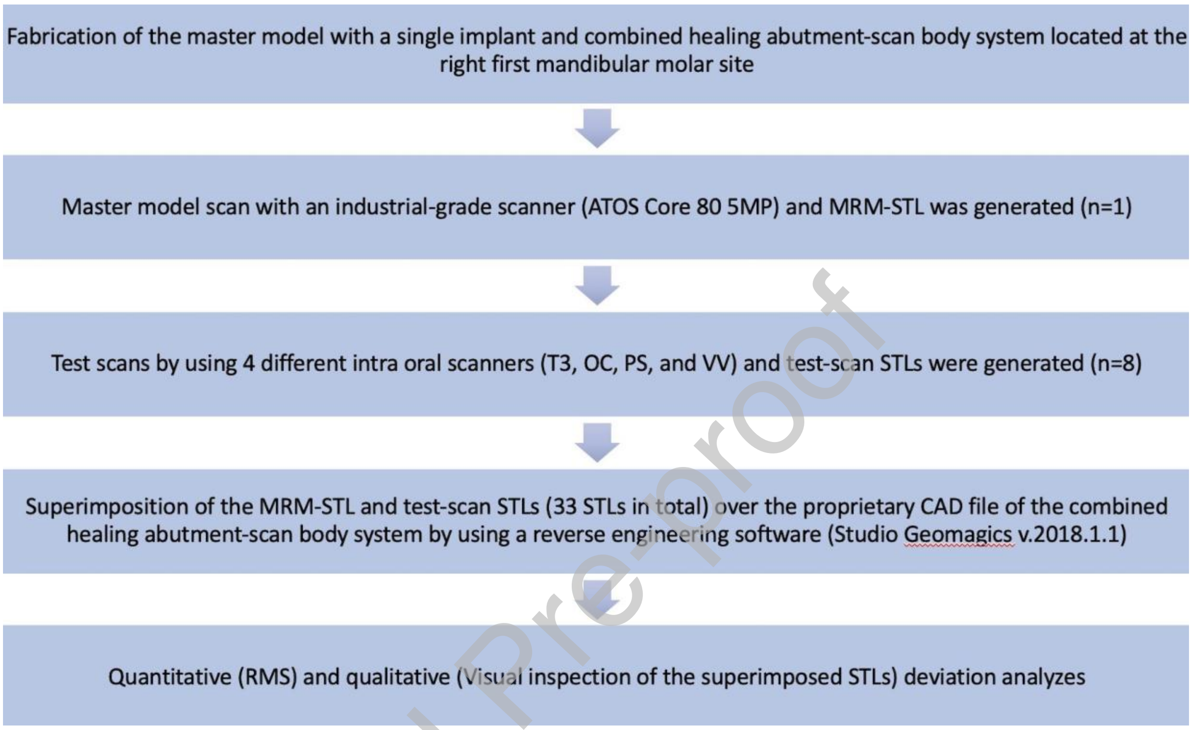

Figure 1. Schematic representation of the study design

Figure 2. Disassembled combined healing abutment-scan body system

Figure 3. Points determined for the alignment procedure (Red: Point on the buccal vertical outdent; Green: Point on the buccal of the triangle located on top of the scan body; Blue:

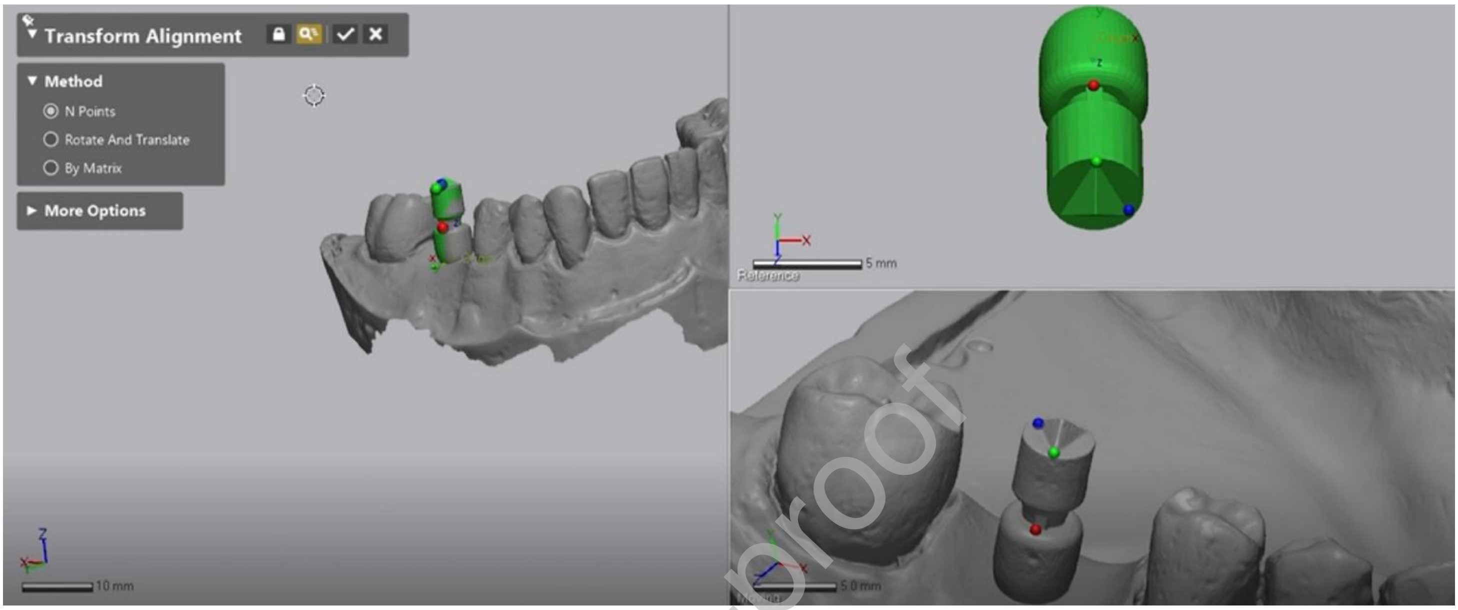

Point on the distal of the triangle located on top of the scan body)

Figure 4. Quantitative evaluation of the CHA-SB system with colorimetric map (A: T3; B: OC; C: PS; D: VV; E; Reference scan; 1: Buccal; 2: Lingual; 3: Occlusal)